








RESEARCH ARTICLE | DECEMBER 18 2023

Kibble–Zurek scaling of nonequilibrium phase transition in barium titanate

Nitish Baradwaj  ; Aravind Krishnamoorthy  ; Ken-ichi Nomura  ; Aiichiro Nakano  ; Rajiv K. Kalia  ; Priya Vashishta  



Appl. Phys. Lett. 123, 252901 (2023)

<https://doi.org/10.1063/5.0176312>



View Online



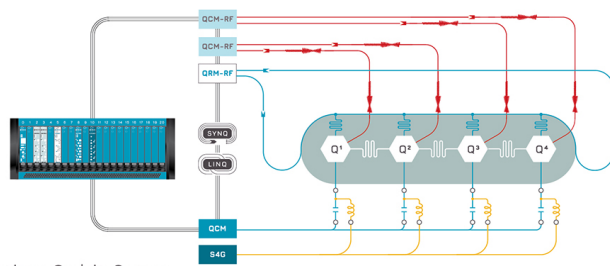
Export Citation

CrossMark



Integrates all Instrumentation + Software for Control and Readout of

Superconducting Qubits
NV-Centers
Spin Qubits



Superconducting Qubit Setup

[find out more >](#)

Kibble–Zurek scaling of nonequilibrium phase transition in barium titanate

Cite as: Appl. Phys. Lett. **123**, 252901 (2023); doi: [10.1063/5.0176312](https://doi.org/10.1063/5.0176312)
 Submitted: 12 September 2023 · Accepted: 30 November 2023 ·
 Published Online: 18 December 2023



View Online



Export Citation



CrossMark

Nitish Baradwaj,¹ Aravind Krishnamoorthy,² Ken-ichi Nomura,¹ Aiichiro Nakano,¹ Rajiv K. Kalia,¹
 and Priya Vashishta^{1,a)}

AFFILIATIONS

¹Collaboratory for Advanced Computing and Simulations, University of Southern California, Los Angeles, California 90089-0242, USA

²Department of Mechanical Engineering, Texas A&M University, College Station, Texas 77843-3123, USA

^{a)} Author to whom correspondence should be addressed: priyav@usc.edu

ABSTRACT

Far-from-equilibrium phase transition dynamics is one of the grand challenges in modern materials science. A theoretical landmark is the Kibble–Zurek (KZ) scaling to describe the relationship between the temperature quenching rate and the resulting defect density in the vicinity of symmetry-breaking phase transformations. Despite the confirmation of the KZ scaling in ferroic perovskite materials and macroscopic simulations, its atomistic mechanisms remain elusive. Here, we demonstrate the KZ scaling using all-atom molecular dynamics simulations for a prototypical ferroelectric perovskite, barium titanate, with the scaling exponent corresponding to the theoretical prediction for rapid quenching. Simulated diffuse neutron scattering data are presented to guide future experiments.

Published under an exclusive license by AIP Publishing. <https://doi.org/10.1063/5.0176312>

The Kibble–Zurek (KZ) mechanism proposes the creation of topological defects due to a continuous second order phase transition driven by a rapid quench rate.^{1–6} Originally in astrophysics and cosmology, the new mechanism was first proposed by Kibble¹ to describe the formation of topological defects in the form of cosmic strings in the early universe, due to rapid temperature quenching as a result of very fast expansion of the universe after the big bang. The KZ transition and generation of topological defects is an inherently nonequilibrium phenomenon; however, a continuous second order phase transition provides an excellent description of the process. The signature of the KZ mechanism is the scaling relation,

$$\xi \propto \tau_q^\sigma, \quad (1)$$

between the length scale ξ of topological defects (\sim separation between defects) and quench time τ_q , where σ is the scaling exponent.^{1,6,7} Though applicability of the KZ mechanism to the early universe was later discarded based on cosmological observations,¹ Zurek investigated these ideas for their applicability to material systems and suggested that the same idea can instead be tested in laboratories for condensed-matter systems.^{3–5} Following Zurek's suggestion, the KZ mechanism has indeed been observed in various materials, with ferroelectric and multiferroic perovskites being some of the most successful examples.^{8–11}

The KZ scaling has been studied theoretically using spin models^{5,12} and macroscopic partial differential equations.^{13,14} More microscopic models, such as coarse-grained molecular dynamics (MD) simulations, have also been applied.¹³ Recently, large-scale atomistic MD simulations on PbTiO₃ perovskite based on a neural-network force field demonstrated KZ-like defect structures under optical quenching instead of temperature quenching. In this work, atomistic processes leading to defect creation and KZ scaling during temperature quenching have not been investigated.¹⁵ We will use large scale MD simulations to demonstrate KZ scaling upon rapid temperature quenching in barium titanate. For our MD simulations, we will use validated reactive force field (ReaxFF) for ferroelectric perovskite barium titanate, BaTiO₃ (BTO) developed by van Duin's group.^{16,17}

Ferroelectric materials, such as BTO, have a wide range of applications as multilayer capacitors, thermistors, and electro-optic devices.^{16–18} In the temperature of interest, BTO occurs in cubic and tetragonal crystal structures (Fig. 1). Electric polarization in BTO stems from this phase change between cubic and tetragonal structures. This phase change occurs when the system is cooled down below 240 K.¹⁹

The ReaxFF used in this study reproduces the experimentally observed transition from the high-temperature cubic non-ferroelectric phase to the low-temperature tetragonal ferroelectric phase at \sim 240 K (Fig. 2).¹⁶ The unit cell of cubic BTO has a lattice constant of 4.01 Å with the mass density of 6.02 g/cm³, and the tetragonal phase has

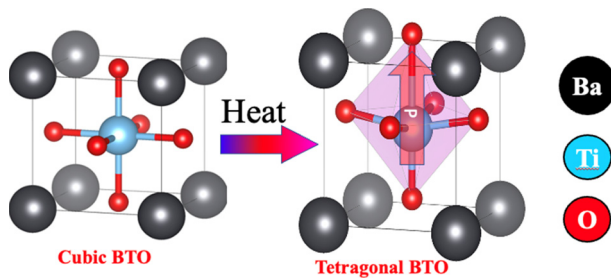


FIG. 1. Two crystal structures of BaTiO_3 . The cubic phase (shown on the left) is non-ferroelectric and shows no net macroscopic polarization, while the tetragonal phase exhibits finite electric polarization because of the asymmetry along c -direction.

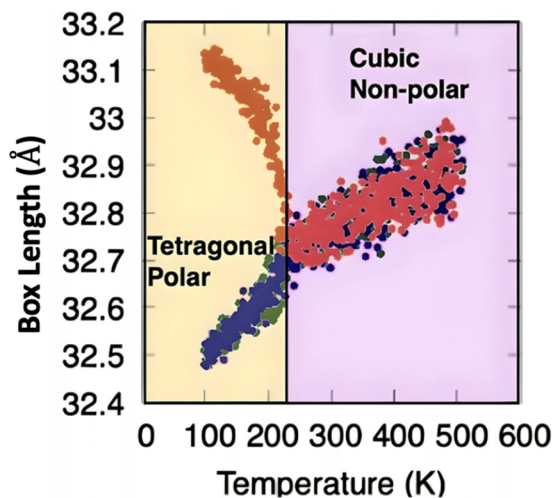


FIG. 2. Variation of molecular dynamics box length of BTO system under cubic to tetragonal phase transformation. As the system is cooled from the non-ferroelectric cubic high temperature phase, the structure transforms to the ferroelectric tetragonal phase.

lattice constants $a=b=3.99 \text{ \AA}$ and $c=4.10 \text{ \AA}$. The details of the forcefields used in the simulations and MD schedule are the following. We perform MD simulations of BTO based on ReaxFF developed by van Duin and collaborators, who have successfully demonstrated the reversible ferroelectric/non-ferroelectric phase transition upon heating and cooling.¹⁶ The force field was trained against various bulk configurations including the equations of state (cubic vs tetragonal phases) and the energetics and migration of oxygen vacancies obtained with first-principles density functional theory (DFT) calculations. The BTO

force field employs the standard ReaxFF form based on the bond-order concept and dynamical atomic charges, and as such, it is easily extendable to a wide variety of other ferroelectric oxides.^{45,46} It provides a computationally inexpensive simulation tool for realistic ferroelectric materials that are highly sensitive to defects, strain, and domain boundaries. Simulations are carried out using the LAMMPS software,⁴⁷ which supports ReaxFF force fields in the LAMMPS/ReaxC package.⁴⁸ While the truncated Coulombic interaction in ReaxFF may not quantitatively describe internal electric fields, it suffices for study of K-Z scaling and its signature in diffuse scattering.

Having validated the structural transformation in BTO as a function of cooling, we now proceed to investigate rate of quenching from high temperature cubic phase to study defect creation and resulting electric polarization.

We generate a high temperature system in the cubic phase of length 200 \AA containing 625 000 atoms. Periodic boundary conditions (PBC) are imposed on the system. The system is gradually heated and thermalized at temperature $T=400 \text{ K}$ in the canonical (NVT) ensemble over 100 000 MD steps with a time step of 1 fs. The thermalized system in the cubic phase is then cooled from 400 K to a temperature of 50 K at different quench rates. The quenching process is carried out using the NPT ensemble in which the simulation box is allowed to change volume and symmetry. The system is quenched to 50 K over $N_{\text{steps}} = 50\,000, 80\,000, 100\,000, 200\,000,$ and $400\,000$ MD steps. Higher number of MD time steps to cool the system down implies a lower quench rate. Simulation workflow of the system is summarized in Fig. 3.

After the completion of the quench, the total dipole moment on the titanium (Ti) atom is calculated for the final configuration by adding the individual dipole moments of the titanium octahedra with its six nearest oxygen (O) atoms. This vector is then normalized, and a state number, +1 or -1, is assigned to each Ti depending on the direction of the vector. A particular titanium atom is classified as a defect if at least one of the six neighboring Ti atoms has a different state number from its own state number. This enables us to compute the defect density.

Figure 4 shows the defect density as a function of the thermal quench rate. Least-square fit of the data gives the scaling exponent of $\sigma = 0.5 \pm 0.02$ in Eq. (1). The exponent in the KZ scaling relation depends on the nature of the thermal fluctuations that are the frozen out.¹⁰ There are two regimes,^{20,21} for which the critical scaling exponent has been calculated, i.e., the mean-field and Ginzburg regimes. In the mean-field regime, thermal fluctuations do not interact with each other, which applies to rapid quench. On the other hand, interactions between fluctuations play a central role in determining the exponent in the Ginzburg regime, which applies to slow quench where the critical slowing down near the phase transition temperature is probed. The value of the KZ exponent in the mean-field regime was determined to



FIG. 3. Workflow for quenching schedule and identifying defects in BTO.

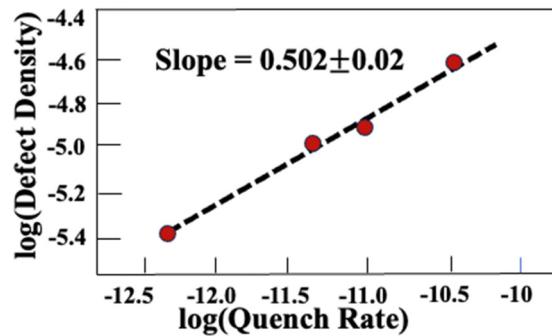


FIG. 4. Variation of defect densities (units of $N_{\text{defects}} \text{ \AA}^{-3}$) in BTO as a function of thermal quench rate in N_{steps}^{-1} (red circles). Dashed line is the least-square fit.

be 0.5,^{1,10,22–24} whereas that in the Ginzburg regime was found to be 0.58.^{9,25–27} The experimental results^{9,28} for RMnO_3 manganites (R denotes a rare-earth element) have found a value of 0.59 close to the Ginzburg value. On the other hand, our MD simulation probes rapid phase-transition dynamics, and accordingly, we observe the mean-field exponent of 0.5.

Neutron diffraction and inelastic scattering are very useful methods for investigating structural and dynamical correlations in

condensed matter systems.^{29–42} The technique is nondestructive because interaction of neutron with atomic nuclei is inherently weak. This allows for an investigation of bulk materials using neutrons, unlike in x-ray scattering where thin samples are required due to strong x-ray absorption in materials. In this paper, we will primarily focus on structural correlations that can be directly measured by neutron diffraction techniques. More specifically, our focus will be on diffuse scattering resulting from defects and imperfections resulting from rapid thermal quenches. Atomistic simulations have played a complementary role in analyzing and understanding the behavior of defects and imperfections in crystalline materials. In addition, large scale atomistic simulations provide a clear path to compute neutron diffuse scattering for a direct comparison with the experimental data.

Figure 5 shows the three-dimensional structure of defects as a function of quench rates. Fastest quench rate is shown on the leftmost figure. In Fig. 6, slices of topological defects are shown as a function of quench rates. Similar to Fig. 5, the fastest quench rate slice is on the left.

We have also computed diffuse neutron scattering (DNS) pattern from these quenched structures to examine the distribution and intensities in the (001) plane (Fig. 7). Our approach relates detailed real-space information on defects to the diffuse neutron scattering data in momentum space. Here, the neutron structure factor $S_N(\mathbf{Q})$ is the total neutron scattering cross section at wave number \mathbf{Q} ,

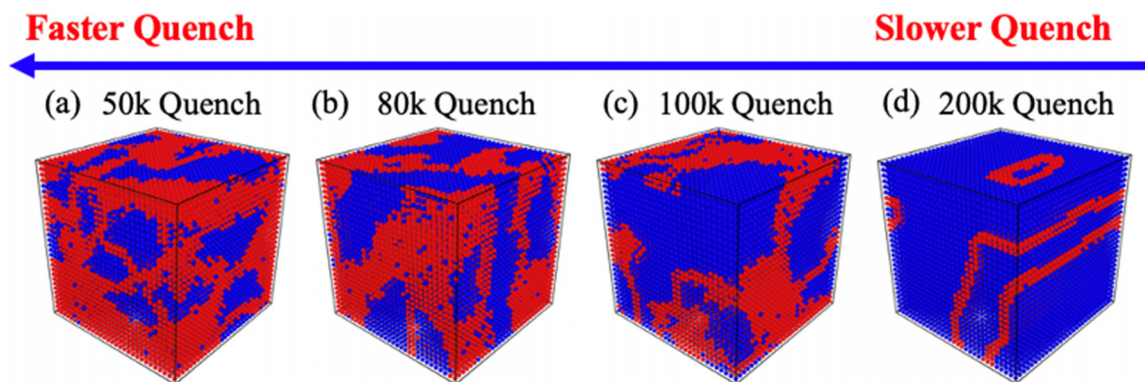


FIG. 5. Real-space defect structure in quenched BTO. The state of the Ti atom is shown from a fast 50k-step quench on the left (a) to a slow 200k-step quench in the right (d). The +1 and -1 states are colored in red and blue, respectively.

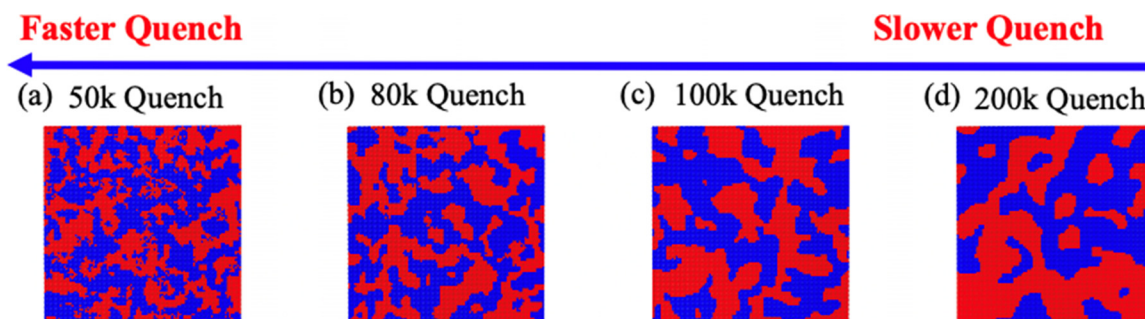


FIG. 6. Slices of the three-dimensional structures shown in Fig. 5 for quenched BTO. As in Fig. 5, we are showing the systems in decreasing quench rates from left to right (a)–(d). The density of defects clearly decreases as we lower the quench rate from 50k steps to 200k steps.

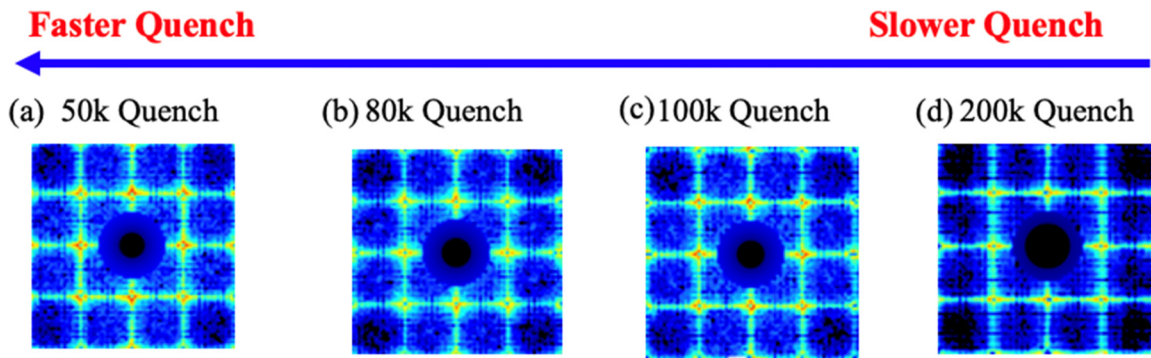


FIG. 7. Computed diffuse scattering in the (001) plane for ferroelectric BTO quenched at four different quench rates: (a) 50k quench—fastest, (b) 80k quench, (c) 100k quench, and (d) 200k quench—slowest. When comparing (a)–(d), it is clear that the diffuse scattering around Bragg peaks (highest intensity marked in red) indicated by yellow region is highest in (a), which corresponds to fastest quench rate and smallest in (d), which corresponds to slowest quench rate.

$$S_N(\mathbf{Q}) = \sum_i \sum_j b_i b_j \exp(i\mathbf{Q} \cdot (\mathbf{R}_i - \mathbf{R}_j)) \exp(i\mathbf{Q} \cdot (\mathbf{u}_i - \mathbf{u}_j)), \quad (2)$$

where b_i , \mathbf{R}_i , and \mathbf{u}_i are the scattering length, position in a perfect crystal, and displacement from the perfect-crystalline position, respectively, for the i th atom.

The key factor in the KZ mechanism is a parameter called the “frozen-out” correlation length ξ . The system goes out of equilibrium at a freeze out time \bar{t} . At longer time scales, the system adiabatically follows close to the transition temperature. Depending on the quench rate, the probed nonequilibrium phase-transition dynamics is reflected by the KZ scaling exponent in Eq. (1), specifically either the mean-field or Ginzburg values. While the rapid quench in our MD simulations for BTO exhibits the former, the frozen defects during the second-order phase transition could eventually be annealed through thermal activation in much longer time, which may be difficult to observe by conventional thermal-quench experiments. Instead, ultrafast pump-probe experiments^{43,44} may be able to detect a similar KZ scaling in an optical-quench setting.¹⁵

We are aware that quenched defect structure in BTO is not stable at room temperature for a long period of time for a diffuse neutron scattering experiment. The goal of our study was to ensure that the defect structure generated in BTO by rapid thermal quench in MD simulations produced KZ scaling consistent with the mean field regime and to establish an experimental connection through diffuse scattering. We are currently investigating YMnO_3 where the defect structure upon rapid thermal quenching is stable at room temperature for the duration months. A joint simulation and diffuse neutron scattering study is being carried out using (1) the CORELLI instrument at Spallation Neutron Source of Oak Ridge National Laboratory and (2) neural-network quantum molecular dynamics simulations to achieve quantum-mechanical accuracy orders-of-magnitude faster, thereby encompassing large experimental length and time scales.

This research was supported by the Scattering and Instrumentation Sciences Program of the Department of Energy, Office of Science, Basic Energy Sciences, under Award No. DE-SC0023146.

AUTHOR DECLARATIONS

Conflict of Interest

The authors have no conflicts to disclose.

Author Contributions

Nitish Baradwaj: Formal analysis (equal); Investigation (equal); Methodology (equal); Software (equal); Validation (equal); Writing – original draft (equal). **Aravind Krishnamoorthy:** Investigation (equal); Methodology (equal); Software (equal); Writing – original draft (equal). **Ken-ichi Nomura:** Investigation (equal); Methodology (equal); Project administration (equal); Resources (equal); Validation (equal); Writing – original draft (equal). **Aiichiro Nakano:** Investigation (equal); Resources (equal); Writing – original draft (equal). **Rajiv K. Kalia:** Investigation (equal); Resources (equal); Writing – original draft (equal). **Priya Vashishta:** Conceptualization (equal); Funding acquisition (equal); Investigation (equal); Supervision (equal); Writing – original draft (equal); Writing – review & editing (equal).

DATA AVAILABILITY

Data sharing is not applicable to this article as no new data were created or analyzed in this study.

REFERENCES

- ¹T. W. B. Kibble, “Phase-transition dynamics in the lab and the universe,” *Phys. Today* **60**(9), 47–52 (2007).
- ²T. W. B. Kibble, “Topology of cosmic domains and strings,” *J. Phys. A: Math. Gen.* **9**(8), 1387–1398 (1976).
- ³W. H. Zurek, “Cosmological experiments in superfluid helium?,” *Nature* **317**(6037), 505–508 (1985).
- ⁴W. H. Zurek, “Cosmological experiments in condensed matter systems,” *Phys. Rep.* **276**(4), 177–221 (1996).
- ⁵W. H. Zurek, U. Dorner, and P. Zoller, “Dynamics of a quantum phase transition,” *Phys. Rev. Lett.* **95**(10), 105701 (2005).
- ⁶H. Kleinert, “From Landau’s order parameter to modern disorder fields,” *AIP Conf. Proc.* **1205**, 103–107 (2010).
- ⁷F. J. Gómez-Ruiz, J. J. Mayo, and A. del Campo, “Full counting statistics of topological defects after crossing a phase transition,” *Phys. Rev. Lett.* **124**(24), 240602 (2020).

- ⁸S. C. Chae, N. Lee, Y. Horibe, M. Tanimura, S. Mori, B. Gao, S. Carr, and S. W. Cheong, "Direct observation of the proliferation of ferroelectric loop domains and vortex-antivortex pairs," *Phys. Rev. Lett.* **108**(16), 167603 (2012).
- ⁹S.-Z. Lin, X. Wang, Y. Kamiya, G.-W. Chern, F. Fan, D. Fan, B. Casas, Y. Z. Liu, V. Kiryukhin, W. H. Zurek *et al.*, "Topological defects as relics of emergent continuous symmetry and Higgs condensation of disorder in ferroelectrics," *Nat. Phys.* **10**(12), 970–977 (2014).
- ¹⁰Q. N. Meier, M. Lilienblum, S. M. Griffin, K. Conder, E. Pomjakushina, Z. Yan, E. Bourret, D. Meier, F. Lichtenberg, E. K. H. Salje *et al.*, "Global formation of topological defects in the multiferroic hexagonal manganites," *Phys. Rev. X* **7**(4), 041014 (2017).
- ¹¹M. Winterer, *Nanocrystalline Ceramics: Synthesis and Structure* (Springer Science & Business Media, 2002).
- ¹²A. Libál and C. J. O. Reichhardt, "Quenched dynamics of artificial colloidal spin ice," *Phys. Rev. Res.* **2**(3), 033433 (2020).
- ¹³Z. Bradač, S. Kralj, and S. Žumer, "Molecular dynamics study of the isotropic-nematic quench," *Phys. Rev. E* **65**(2), 021705 (2002).
- ¹⁴W. Wen, S. Zhu, Y. Xie, B. Ou, W. Wu, P. Chen, M. Gong, and G. Guo, "Generalized Kibble-Zurek mechanism for defects formation in trapped ions," *Sci. China: Phys. Mech., Astron.* **66**(8), 280311 (2023).
- ¹⁵T. Linker, K. Nomura, A. Aditya, S. Fukushima, R. K. Kalia, A. Krishnamoorthy, A. Nakano, P. Rajak, K. Shimmura, F. Shimojo, and P. Vashishta, "Exploring far-from-equilibrium ultrafast polarization control in ferroelectric oxides with excited-state neural network quantum molecular dynamics," *Sci. Adv.* **8**(12), eabk2625 (2022).
- ¹⁶D. Akbarian, D. E. Yilmaz, Y. Cao, P. Ganesh, I. Dabo, J. Munro, R. Van Ginhoven, and A. C. T. van Duin, "Understanding the influence of defects and surface chemistry on ferroelectric switching: A ReaxFF investigation of BaTiO₃," *Phys. Chem. Chem. Phys.* **21**(33), 18240–18249 (2019).
- ¹⁷W. Preis, "Modeling oxygen diffusion in barium titanate using molecular dynamics: Comparison between Mg and Sc dopants," *J. Phys. Chem. Solids* **181**, 111525 (2023).
- ¹⁸F. Chen, Y. Zhu, S. Liu, Y. Qi, H. Y. Hwang, N. C. Brandt, J. Lu, F. Quirin, H. Enquist, P. Zalden *et al.*, "Ultrafast terahertz-field-driven ionic response in ferroelectric BaTiO₃," *Phys. Rev. B* **94**(18), 180104 (2016).
- ¹⁹M. B. Smith, K. Page, T. Siegrist, P. L. Redmond, E. C. Walter, R. Seshadri, L. E. Brus, and M. L. Steigerwald, "Crystal structure and the paraelectric-to-ferroelectric phase transition of nanoscale BaTiO₃," *J. Am. Chem. Soc.* **130**(22), 6955–6963 (2008).
- ²⁰L. Landau and I. Khalatnikov, "Ob anomal'nom pogloshchenii zvuka vblizi tochek fazovo perekhoda vtorovo roda," *Dokl. Akad. Nauk SSSR* **96**, 469 (1954).
- ²¹L. D. Landau and E. M. Lifshitz, *Fluid Mechanics: Landau and Lifshitz: Course of Theoretical Physics* (Elsevier, 2013), Vol. 6.
- ²²P. C. Hohenberg and A. P. Krekhov, "An introduction to the Ginzburg–Landau theory of phase transitions and nonequilibrium patterns," *Phys. Rep.* **572**, 1–42 (2015).
- ²³E. Salje, "Kinetic rate laws as derived from order parameter theory I: Theoretical concepts," *Phys. Chem. Miner.* **15**(4), 336–348 (1988).
- ²⁴E. K. Salje, "Application of Landau theory for the analysis of phase transitions in minerals," *Phys. Rep.* **215**(2), 49–99 (1992).
- ²⁵M. Lilienblum, T. Lottermoser, S. Manz, S. M. Selbach, A. Cano, and M. Fiebig, "Ferroelectricity in the multiferroic hexagonal manganites," *Nat. Phys.* **11**(12), 1070–1073 (2015).
- ²⁶D. R. Nelson, "Coexistence-curve singularities in isotropic ferromagnets," *Phys. Rev. B* **13**(5), 2222–2230 (1976).
- ²⁷M. Oshikawa, "Ordered phase and scaling in Z_n models and the three-state antiferromagnetic Potts model in three dimensions," *Phys. Rev. B* **61**(5), 3430–3434 (2000).
- ²⁸R. Monaco, M. Aaroe, J. Mygind, R. Rivers, and V. Koshelets, "Experiments on spontaneous vortex formation in Josephson tunnel junctions," *Phys. Rev. B* **74**(14), 144513 (2006).
- ²⁹R. Pynn, "Neutron scattering by rough surfaces at grazing incidence," *Phys. Rev. B* **45**(2), 602–612 (1992).
- ³⁰P. Müller-Buschbaum, E. Metwalli, J. F. Moulin, V. Kudryashov, M. Haese-Seiller, and R. Kampmann, "Time of flight grazing incidence small angle neutron scattering," *Eur. Phys. J. Spec. Top.* **167**(1), 107–112 (2009).
- ³¹I. A. Zaliznyak, A. T. Savici, V. Ovidiu Garlea, B. Winn, U. Filges, J. Schneeloch, J. M. Tranquada, G. Gu, A. Wang, and C. Petrovic, "Polarized neutron scattering on HYSPEC: The HYbrid SPECtrometer at SNS," *J. Phys.: Conf. Ser.* **862**(1), 012030 (2017).
- ³²M. Doucet, A. M. Samarakoon, C. Do, W. T. Heller, R. Archibald, D. A. Tennant, T. Proffen, and G. E. Granroth, "Machine learning for neutron scattering at ORNL," *Mach. Learn.: Sci. Technol.* **2**(2), 023001 (2021).
- ³³J. K. Zhao, C. Y. Gao, and D. Liu, "The extended Q-range small-angle neutron scattering diffractometer at the SNS," *J. Appl. Crystallogr.* **43**(5), 1068–1077 (2010).
- ³⁴W. T. Heller, M. Cuneo, L. Debeer-Schmitt, C. Do, L. He, L. Heroux, K. Littrell, S. V. Pingali, S. Qian, C. Stanley *et al.*, "The suite of small-angle neutron scattering instruments at Oak Ridge National Laboratory," *J. Appl. Crystallogr.* **51**(2), 242–248 (2018).
- ³⁵G. Shirane, "Neutron scattering studies of structural phase transitions at Brookhaven," *Rev. Mod. Phys.* **46**(3), 437 (1974).
- ³⁶B. J. Kennedy, C. J. Howard, and B. C. Chakoumakos, "Phase transitions in perovskite at elevated temperatures—A powder neutron diffraction study," *J. Phys.: Condens. Matter* **11**(6), 1479 (1999).
- ³⁷L. Schmidt-Mende, V. Dyakonov, S. Olthof, F. Ünlü, K. M. T. Lê, S. Mathur, A. D. Karabanov, D. C. Lupascu, L. M. Herz, A. Hinderhofer *et al.*, "Roadmap on organic–inorganic hybrid perovskite semiconductors and devices," *APL Mater.* **9**(10), 109202 (2021).
- ³⁸M. J. Krogstad, P. M. Gehring, S. Rosenkranz, R. Osborn, F. Ye, Y. Liu, J. P. Ruff, W. Chen, J. M. Wozniak, and H. Luo, "The relation of local order to material properties in relaxor ferroelectrics," *Nat. Mater.* **17**(8), 718–724 (2018).
- ³⁹D. A. Tennant, "Studies of spinons, Majoranas, and monopoles in spin liquid and quantum critical magnets with neutrons," *J. Phys. Soc. Jpn.* **88**(8), 081009 (2019).
- ⁴⁰B. Li, D. Louca, J. Niedziela, Z. Li, L. Zhang, J. Zhou, and J. B. Goodenough, "Lattice and magnetic dynamics in perovskite $Y_{1-x}La_xTiO_3$," *Phys. Rev. B* **94**(22), 224301 (2016).
- ⁴¹B. Li, D. Louca, S. Yano, L. G. Marshall, J. Zhou, and J. B. Goodenough, "Insulating pockets in metallic $LaNiO_3$," *Adv. Elect. Mater.* **2**(2), 1500261 (2016).
- ⁴²P. Tong, D. Louca, N. Lee, and S. W. Cheong, "Oxygen displacements and magneto-electric coupling in $LuMnO_3$," *Phys. Rev. B* **86**(9), 094419 (2012).
- ⁴³M. F. Lin, V. Kochat, A. Krishnamoorthy, L. Bassman, C. Weninger, Q. Zheng, X. Zhang, A. Apte, C. S. Tiwary, X. Z. Shen *et al.*, "Ultrafast non-radiative dynamics of atomically thin $MoSe_2$," *Nat. Commun.* **8**, 1745 (2017).
- ⁴⁴I. Tung, A. Krishnamoorthy, S. Sadasivam, H. Zhou, Q. Zhang, K. L. Seyler, G. Clark, E. M. Mannebach, C. Nyby, F. Ernst *et al.*, "Anisotropic structural dynamics of monolayer crystals revealed by femtosecond surface x-ray scattering," *Nat. Photonics* **13**, 425–430 (2019).
- ⁴⁵A. C. T. van Duin, S. Dasgupta, F. Lorant, and W. A. Goddard, "ReaxFF: A reactive force field for hydrocarbons," *J. Phys. Chem. A* **105**(41), 9396–9409 (2001).
- ⁴⁶K. Nomura, R. K. Kalia, A. Nakano, P. Vashishta, A. C. T. van Duin, and W. A. Goddard, "Dynamic transition in the structure of an energetic crystal during chemical reactions at shock front prior to detonation," *Phys. Rev. Lett.* **99**(14), 148303 (2007).
- ⁴⁷A. P. Thompson, H. M. Aktulga, R. Berger, D. S. Bolintineanu, W. M. Brown, P. S. Crozier, P. J. in't Veld, A. Kohlmeyer, S. G. Moore, T. D. Nguyen *et al.*, "LAMMPS—A flexible simulation tool for particle-based materials modeling at the atomic, meso, and continuum scales," *Comput. Phys. Commun.* **271**, 108171 (2022).
- ⁴⁸K. Chenoweth, A. C. Van Duin, and W. A. Goddard, "ReaxFF reactive force field for molecular dynamics simulations of hydrocarbon oxidation," *J. Phys. Chem. A* **112**(5), 1040–1053 (2008).